A new attraction-detachment model for explaining flow sliding in clay-rich tephras

Kluger, Max O.
Moon, Vicki G.
Kreiter, Stefan
Lowe, David J.
Churchman, G. J.
Hepp, Daniel A.
Seibel, David
Jorat, M. Ehsan
Mörz, Tobias

Publisher: GSA
Journal: GEOL: Geology
DOI:10.1130/G38560.1

A new attraction-detachment model for explaining flow sliding in clay-rich tephras

Max O. Kluger[1], Vicki G. Moon[2], Stefan Kreiter[1], David J. Lowe[2], G.J. Churchman[3], Daniel A. Hepp[1], David Seibel[1], M. Ehsan Jorat[4], and Tobias Mörz[1]

[1]Marum – Center for Marine Environmental Sciences, University of Bremen, Leobener Straße, 28359 Bremen, Germany

[2]School of Science, University of Waikato, Private Bag 3105, Hamilton 3240, New Zealand

[3]School of Agriculture, Food and Wine, University of Adelaide, Adelaide 5005, Australia

[4]School of Science, Engineering and Technology, Abertay University, Dundee, DD11HG, UK

ABSTRACT

Altered pyroclastic (tephra) deposits are highly susceptible to landsliding, leading to fatalities and property damage every year. Halloysite, a low-activity clay mineral, is often associated with landslide-prone layers within altered tephra successions, especially in deposits with high sensitivity, which describes the post-failure strength loss. However, the precise role of halloysite in the development of sensitivity, and thus in sudden and unpredictable landsliding, is unknown. Here we show that an abundance of mushroom-cap-shaped (MCS) spheroidal halloysite governs the development of sensitivity, and hence proneness to landsliding, in altered rhyolitic tephras, North Island, New Zealand. We found that a highly sensitive layer, which was involved in a flow slide, has a remarkably high content of aggregated MCS spheroids with substantial openings on one

side. We suggest that short-range electrostatic and van der Waals' interactions enabled the MCS spheroids to form interconnected aggregates by attraction between the edges of numerous paired silanol and aluminol sheets that are exposed in the openings and the convex silanol faces on the exterior surfaces of adjacent MCS spheroids. If these weak attractions are overcome during slope failure, multiple, weakly-attracted MCS spheroids can be separated from one another and the prevailing repulsion between exterior MCS surfaces results in a low remolded shear strength, a high sensitivity, and a high propensity for flow sliding. The evidence indicates that the attraction-detachment model explains the high sensitivity and contributes to an improved understanding of the mechanisms of flow sliding in sensitive, altered tephras rich in spheroidal halloysite.

INTRODUCTION

Most East Asian and western Pacific countries are located in tectonically active, high-rainfall areas where landslides are a major natural hazard. These landslides are typically triggered by rainstorms or earthquakes, and are responsible for fatalities and enormous property damage every year. Many destructive landslides have occurred in pyroclastic deposits in Japan, Indonesia, Hong Kong, and New Zealand (Chau et al., 2004; Chigira, 2014; Moon, 2016), such deposits often containing layers rich in clay minerals formed mainly by chemical weathering either during pedogenesis or diagenesis. In regions with predominantly rhyolitic volcanism, halloysite is a common clay mineral (Churchman and Lowe, 2012) and is therefore potentially a key geological factor increasing the risk of landslides (Kirk et al., 1997; Chigira, 2014). Halloysite is a 1:1 Si:Al layered aluminosilicate member of the kaolin subgroup that exhibits various structural morphologies including tubes, spheroids, polyhedrons, plates and books (Joussein et al., 2005; Cunningham et al., 2016).

Spheroidal halloysite, in particular, has been recognized in landslide-prone layers of pyroclastic material in Japan (Tanaka, 1992) and New Zealand (Smalley et al., 1980). Smalley et al. (1980) linked a high content of spheroidal halloysite to high sensitivity. Sensitivity refers to the post-failure strength loss in the failure zone during landsliding, and is quantified in the laboratory as the ratio of the undisturbed to remolded undrained shear strength at the same water content (Terzaghi, 1944). High sensitivities were first described for post-glacial, brackish and marine clayey sediments in the Northern Hemisphere (Skemption and Northey, 1952) that are subject to landslides with dimensions and long runout distances difficult to predict. In this study, we investigate processes that have led to high sensitivity in halloysite-rich pyroclastic materials in order to improve landslide-hazard evaluation.

GEOLOGICAL SETTING

Much of the central part of New Zealand's North Island is covered by thick rhyolitic tephras (Lowe, 2011) derived from eruptions in the Taupo Volcanic Zone (Briggs et al., 2005), which are often altered into halloysite-rich successions. We focus here on a coastal flow slide at Omokoroa, Bay of Plenty (Fig. 1A), where ~10,000 m^3 of material were transported downslope over long distance into a lagoon in 1979 (Moon et al., 2015), as well as two minor reactivations in 2011 and 2012. The 1979 event was likely initiated in a white, highly sensitive layer with high spheroidal halloysite concentration (Smalley et al., 1980), lacking any detectable allophane (Cunningham et al., 2016).

DOI:10.1130/G38560.1

We have analyzed a 40 m-long sediment core, *Omok-1*, which was bored via rotary flush drilling in unfailed material near the headwall (Fig. 1B). The lithology of *Omok-1* was determined by correlation with units of a previously-studied adjacent headwall face (Moon et al., 2015) comprising a succession mainly of Quaternary rhyolitic tephras: overlying lignite at the base of the core, the Pahoia Tephra sequence includes the Te Puna ignimbrite (~0.93 Ma), and a series of altered tephras, which are informally divided into lower and upper Pahoia Tephra units based on two distinct paleosols (P1 and P3). All these deposits and paleosols are overlain by successions of younger altered tephras called Hamilton Ash beds (~0.35 to ~0.05 Ma) and late Quaternary tephras (<~0.05 Ma) (Fig. 1C and 2A). The lower Pahoia Tephras include the 0.3-m-thick, white, highly sensitive clay-rich layer which failed in 1979 (Fig. 1C), having high porosity and high natural water content (Smalley et al., 1980).

METHODS

We performed laboratory vane shear tests on samples from the Pahoia Tephra sequence and Hamilton Ash beds to measure the sensitivity *S*:

$$S = s_u / s_r \quad (1)$$

where the undisturbed strength (s_u) was measured on the intact surface of the split core, and the remolded strength (s_r) was measured on core samples with the same water content, which have been kneaded by hand for 10 min (Jacquet, 1990). Halloysite concentration in bulk samples was measured by X-ray diffraction (XRD) using a Philips PW analytical defractometer and quantification was performed using QUAX (Vogt et al., 2002). Scanning electron microscopy (SEM) was undertaken with a Zeiss Supra40 microscope on 24 shock-frozen, freeze-dried, and gold-coated bulk core samples (Reed, 2005). The relative abundances of halloysite particles having distinct morphologies were quantified using a point-counting approach (Frolov and Maling, 1969). Six representative SEM-images of planar soil surfaces were chosen for each sample and at least 600 particles were counted based on rectangular grids. In the white, highly sensitive layer, the change of halloysite particle arrangement upon remolding was quantified by comparing 20 SEM images of undisturbed and remolded material, providing > 1000 counts, respectively. The spheroid diameters were measured from six representative particles per SEM image.

HIGHLY SENSITIVE SLIDE-PRONE LAYER DOMINATED BY SPHEROIDAL HALLOYSITE

The sensitivity is low in the upper Pahoia Tephras, especially in the paleosols P2 and P3 (Fig. 2A, B). However, the sensitivity tends to increase with depth, reaching values of 15–20 in the lower Pahoia Tephras. The highest sensitivity (Rosenqvist, 1953) of $S = 55$, and the lowest remolded shear strength within the profile of $s_r = 1.4$ kPa, were measured in the white, highly sensitive layer at 23 m depth.

The upper Pahoia Tephras have a halloysite content of 10–20 wt.%, and are comprised almost entirely of tubular halloysite (Fig. 2C, D). The lower Pahoia Tephras have 40–50 wt.% halloysite comprising mostly spheroidal particles. In the highly sensitive layer, 76% of the halloysite is spheroidal, and the spheroid sizes are greater than those in the surrounding layers (Fig. 2D). The 3D line plot reveals a clear correlation between high sensitivities and high halloysite bulk concentration, and a high content of spheroids with large diameters (Fig. 2F). The high sensitivity is associated with low remolded shear strength rather than with high undisturbed shear strength (Fig. 2G).

We found that deposits with high tubular halloysite content hampered sensitivity development, whereas halloysite spheroids facilitate sensitivity and dominate the highly sensitive layer at 23 m depth within the lower Pahoia Tephras. The highly sensitive layer has low remolded shear strength consequent after failure, which, together with its high water content (Smalley et al., 1980), partly contributed to the long runout distance of the flow slide at Omokoroa.

NEW HALLOYSITE MORPHOLOGY

We present here first observations of a previously unreported halloysite particle morphology that is visible in the SEM images of the remolded halloysite fabrics of the highly sensitive layer. In the undisturbed state, the spheroidal halloysites are distinctly aggregated into networks of well-connected particles (Fig. 3E, F). After remolding, however, most of the aggregates have broken apart into small, loose clusters or individual halloysite particles that are typically ~250–400 nm in diameter (Fig. 3G, H). Individual spheroids have distinctive 'deformities' in the form of openings ~80–160 nm in diameter on one side. These openings were previously hidden by contact with other spheroids. The deformities give the particles an ovate "mushroom-cap" appearance. Point-counting individual mushroom-caps in both undisturbed (aggregated) and remolded (disaggregated) samples showed that the observable mushroom-caps were much more abundant in the remolded samples, increasing from 4.4 ± 3.2% to 44.9 ± 11.6%.

ATTRACTION-DETACHMENT MODEL FOR FLOW SLIDING IN ALTERED TEPHRAS

The open-sided, mushroom-cap-shaped halloysite morphology has not been reported previously. Because this particular morphology overwhelmingly occurs in the highly sensitive slide-prone layer, we hypothesize that this unique particle shape controls the mechanical behavior of halloysite clays.

Halloysite is composed of an Al-octahedral (aluminol) sheet with a net positive charge and a Si-tetrahedral (silanol) sheet with a net negative charge at pH values between ~2 and ~8 (Fig. 3I) (Churchman et al., 2016). The two sheets have slightly different dimensions, with the silanol sheet being larger. This misfit in the sheet sizes causes the halloysite layer to be curved (Churchman and Lowe, 2012), with the larger negatively-charged silanol sheet on the outside of the curvature and the positively-charged smaller aluminol sheet on the inside. The halloysite spheroids observed in our study are most likely composed of concentrically stacked 1:1 layers, i.e., with an onion-like structure, as shown in numerous studies including those on spheroidal halloysite derived from altered tephras in New Zealand, Japan, and Argentina (Wada et al., 1977; Kirkman, 1981; Cravero et al., 2012; Berthonneau et al., 2015). For a perfect halloysite spheroid, the outermost silanol surface carries a net negative charge and hence the electrostatic interactions between individual spheroids would be repulsive (Fig. 3I). Our study shows, however, a halloysite structure where both silanol and aluminol layers are exposed at spheroid openings and therefore charges within the openings would correspondingly be weakly positive or neutral overall (Fig. 3J), as indicated from charge density-functional tight-binding modeling applied to halloysite nanotubes (Guimarães et al., 2010). If sufficient numbers of positively charged openings are exposed, the electrostatic interactions between them and the negative exterior silanol surfaces would allow the mushroom-cap-shaped spheroids to form stacked aggregates (Fig. 3K). If the paired silanol and aluminol sheets exposed in the openings are neutral overall, then a net increase in particle attraction will still occur because electrostatic repulsion is reduced and the larger contact areas lead to higher van der Waals' forces (Israelachvili, 2011).

During diagenesis via hydrolysis of volcanic glass (Cunningham et al., 2016), the halloysite spheroids may form consecutively on top of one another in pore spaces, generating the distinct openings during synthesis. The attractive forces between the openings and the convex exterior surfaces are demonstrably strong enough to allow for the formation of aggregates, but also permit easy disaggregation by mechanical detachment during shear (Fig. 3L). New random contacts between convex silanol surfaces probably lead to a decrease in average attraction between particles. We posit that the detachment of attractive spheroidal particle contacts, in the presence of abundant water having negligible interaction with soil-water ions because of the inactive nature of halloysite (Smalley et al., 1980), leads to the very low post-failure shear strength, facilitating a flow slide with long runout distance. The interparticle, attraction-detachment model appears to successfully explain (at nanoscale dimensions) the post-failure behavior of the highly sensitive tephra layer at Omokoroa that is dominated by the imperfect halloysite spheroids. The question therefore arises if similar altered tephras elsewhere have high contents of spheroidal halloysite with potentially hidden mushroom-cap forms, and if such forms helped mobilize other landslides in the past.

CONCLUSIONS

We investigated a sequence of altered, rhyolitic Quaternary tephras in New Zealand, and the reasons why a landslide-prone layer dominated by spheroidal halloysite was highly sensitive. We explain this high sensitivity with an electrostatic attraction-detachment model. Weakly positive or neutral charges on silanol and aluminol sheet edges exposed in the concave openings of spheroidal halloysite particles were attracted to the negatively-charged convex silanol surfaces of adjacent spheroids. Such short-range attractions between spheroid openings, and the exterior surfaces of adjacent spheroids, stabilize an aggregated halloysite framework. If the aggregates are detached by remolding, the loose arrangement of the spheroids exhibits low remolded shear strength. We suggest that the attraction-detachment model, based on the identification of mushroom-cap halloysite morphologies, provides a potential key for the identification of sensitive altered tephras that are predisposed to sudden failure that triggers landsliding.

ACKNOWLEDGMENTS

This research was funded by the DFG-Research Center MARUM (Bremen University) through INTERCOAST and University of Waikato. We thank C. Schulze for vane shear tests, B. Steinborn and C. Vogt for XRD analyses, P. Witte, A. Hübner, C. Schott, S. Buchheister, and V. Diekamp for laboratory assistance, M. Ikari, F. Sense, J. Lane, and P. Pasbakhsh for comments, and F. Terrible, J. K. Torrance, F. Cravero, M. McSaveney, and an anonymous expert, for helpful reviews.

REFERENCES CITED

Berthonneau, J., Grauby, O., Jeannin, C., Chaudanson, D., Joussein, E., and Baronnet, A., 2015, Native morphology of hydrated spheroidal halloysite observed by environmental transmission electron microscopy: Clays and Clay Minerals, v. 63, p. 368–377, doi:10.1346/CCMN.2015.0630503.

Briggs, R., Houghton, B., McWilliams, M., and Wilson, C., 2005, 40Ar/39Ar ages of silicic volcanic rocks in the Tauranga-Kaimai area, New Zealand: dating the transition between volcanism in the Coromandel Arc and the Taupo Volcanic Zone:

New Zealand Journal of Geology and Geophysics, v. 48, p. 459–469, doi:10.1080/00288306.2005.9515126.

Chau, K., Sze, Y., Fung, M., Wong, W., Fong, E., and Chan, L., 2004, Landslide hazard analysis for Hong Kong using landslide inventory and GIS: Computers & Geosciences, v. 30, p. 429–443, doi:10.1016/j.cageo.2003.08.013.

Chigira, M., 2014, Geological and geomorphological features of deep-seated catastrophic landslides in tectonically active regions of Asia and implications for hazard mapping: Episodes, v. 37, p. 284–294.

Churchman, G.J., and Lowe, D.J., 2012, Alteration, formation, and occurrence of minerals in soils, *in* Huang, P. M., Li, Y., and Sumner, M. E., eds., Handbook of Soil Sciences. Properties and Processes, 2nd edition: Boca Raton, Florida, CRC Press, p. 20.21–20.72.

Churchman, G.J., Pasbakhsh, P., Lowe, D.J., and Theng, B.K.G., 2016, Unique but diverse: some observations on the formation, structure, and morphology of halloysite: Clay Minerals, v. 51, p. 395-416, doi:10.1180/claymin.2016.051.3.16.

Cravero, F., Maiza, P., and Marfil, S., 2012, Halloysite in Argentinian deposits: origin and textural constraints: Clay Minerals, v. 47, p. 329–340, doi:10.1180/claymin.2012.047.3.04.

Cunningham, M. J., Lowe, D. J., Wyatt, J. B., Moon, V. G., and Jock Churchman, G., 2016, Discovery of halloysite books in altered silicic Quaternary tephras, northern New Zealand: Clay Minerals, v. 51, p. 351-372, doi:10.1180/claymin.2016.051.3.16.

Frolov, Y., and Maling, D., 1969, The accuracy of area measurement by point counting techniques: The Cartographic Journal, v. 6, p. 21–35, doi:10.1179/caj.1969.6.1.21.

Guimarães, L., Enyashin, A.N., Seifert, G., and Duarte, H.A., 2010, Structural, electronic, and mechanical properties of single-walled halloysite nanotube models: The Journal of Physical Chemistry C, v. 114, p. 11358–11363, doi:10.1021/jp100902e.

Israelachvili, J.N., 2011, Intermolecular and Surface Forces (3rd Edition): Waltham, Massachusetts, Academic Press, 704 p.

Jacquet, D., 1990, Sensitivity to remoulding of some volcanic ash soils in New Zealand: Engineering Geology, v. 28, p. 1–25, doi:10.1016/0013-7952(90)90031-U.

Joussein, E., Petit, S., Churchman, J., Theng, B., Righi, D., and Delvaux, B., 2005, Halloysite clay minerals—a review: Clay Minerals, v. 40, p. 383–426, doi:10.1180/0009855054040180.

Kirk, P., Campbell, S., Fletcher, C., and Merriman, R., 1997, The significance of primary volcanic fabrics and clay distribution in landslides in Hong Kong: Journal of the Geological Society, v. 154, p. 1009–1019, doi:10.1144/gsjgs.154.6.1009.

Kirkman, J.H., 1981, Morphology and structure of halloysite in New Zealand tephras: Clays and Clay Minerals, v. 29, p. 1–9, doi:10.1346/CCMN.1981.0290101.

Lowe, D.J., 2011, Tephrochronology and its application: a review: Quaternary Geochronology, v. 6, p. 107–153, doi:10.1016/j.quageo.2010.08.003.

Moon, V.G., Lowe, D.J., Cunningham, M.J., Wyatt, J.B., de Lange, W.P., Churchman, G.J., Mörz, T., Kreiter, S., Kluger, M.O., and Jorat, M.E., 2015, Sensitive pyroclastic-derived halloysitic soils in northern New Zealand: interplay of microstructure, minerals, and geomechanics, in Rotonda, T. et al., eds.,Volcanic Rocks and Soils. Proceedings of the International Workshop on Volcanic Rocks and Soils, Lacco Ameno, Ischia Island, Italy: London, Taylor and Francis, p. 3–21.

Moon, V., 2016, Halloysite behaving badly: geomechanics and slope behaviour of halloysite-rich soils: Clay Minerals, v. 51, p. 517-528, doi:10.1180/claymin.2016.051.3.09.

Reed, S.J.B., 2005, Electron Microprobe Analysis and Scanning Electron Microscopy in Geology: Cambridge, UK, Cambridge University Press, 212 p, doi:10.1017/CBO9780511610561.

Rosenqvist, I.T., 1953, Considerations on the sensitivity of Norwegian quick-clays: Geotechnique, v. 3, p. 195–200, doi:10.1680/geot.1953.3.5.195.

Skemption, A., and Northey, R., 1952, The sensitivity of clays: Geotechnique, v. 3, p. 30–53, doi:10.1680/geot.1952.3.1.30.

Smalley, I., Ross, C.W., and Whitton, J., 1980, Clays from New Zealand support the inactive particle theory of soil sensitivity: Nature, v. 288, p. 576–577, doi:10.1038/288576a0.

Tanaka, K., 1992, Slope hazards and clay minerals: Nendo Kagaku, v. 32, p. 16–22.

Terzaghi, K., 1944, Ends and Means in Soil Mechanics: Engineering Journal, v. 27, p. 608–615.

Vogt, C., Lauterjung, J., and Fischer, R.X., 2002, Investigation of the clay fraction (< 2 μm) of the Clay Minerals Society Reference Clays: Clays and Clay Minerals, v. 50, p. 388–400, doi:10.1346/000986002760833765.

Wada, S.-I.-, Aoki, K., and Wada, K., 1977, The interior structure of spherical halloysite particles: Clay Science, v. 5, p. 113–121.

FIGURE CAPTIONS

Figure 1. A: Map of Tauranga Harbour, New Zealand, with the Taupo Volcanic Zone (TVZ) as main source for Quaternary tephras at the study site. B: 3D-view of the Bramley Drive flow slide at Omokoroa; red line marks the position of the profile in C. C: Profile through the flow slide with simplified stratigraphy and associated paleosols (P1–4) of core *Omok-1* and ages (in Ma) after Moon et al. (2015).

Figure 2. A: Stratigraphy of core *Omok-1* after Moon et al. (2015) showing the main lithological units as defined in Figure 1, three paleosols (P1–3), and the highly sensitive white layer at 23-m depth (hatched area). B: Undisturbed (s_u) and remolded (s_r) shear strength, and sensitivity (S). C: Halloysite bulk concentration. D: Cumulative volume % (c. %) of halloysite morphologies with bars indicating average standard deviations. E: Average spheroid sizes with standard deviations depicted by fill patterns. F: 3D line plot illustrating the relationship between spheroid content, sensitivity, spheroid size, and halloysite concentration; gray graded areas enable trends in sensitivity to be visualized. G: Dependency between sensitivity and shear strength.

Figure 3. SEM-images of spheroids (A), polyhedrons (B), tubes (C), and plates (D) representing the main halloysite morphologies in the Pahoia Tephra sequence. SEM-images from the highly sensitive layer of undisturbed and multiply connected halloysite spheroids (E, F) and remolded spheroids (G, H) showing smaller clusters or detached spheroids within a much looser particle network. 1: Exposed layers in spheroid openings. 2: Partially separated halloysite spheroids. 3: Detached mushroom-cap-shaped halloysite

DOI:10.1130/G38560.1

spheroid. I: Electrostatic field proximal to halloysite nanotubes with colored equipotential surfaces (ES), modified with permission from Guimarães et al. (2010). Copyright 2010 American Chemical Society. J: Conceptual mushroom-cap-shaped spheroid cross-section and the weak electrostatic and/or van der Waals’ attractions arising between the exposed silanol-aluminol sheets in spheroid openings and the negatively-charged convex exterior surfaces; enlargement is adapted from Berthonneau et al. (2015). Circles with + and – relate to the positive and negative electrostatic field proximal to the spheroid’s exterior surface. Mushroom-cap-shaped spheroids connect with one another between concave openings and convex outer spheroid surfaces, forming aggregates (K) which are partly detached because of remolding (L).

Figure 1

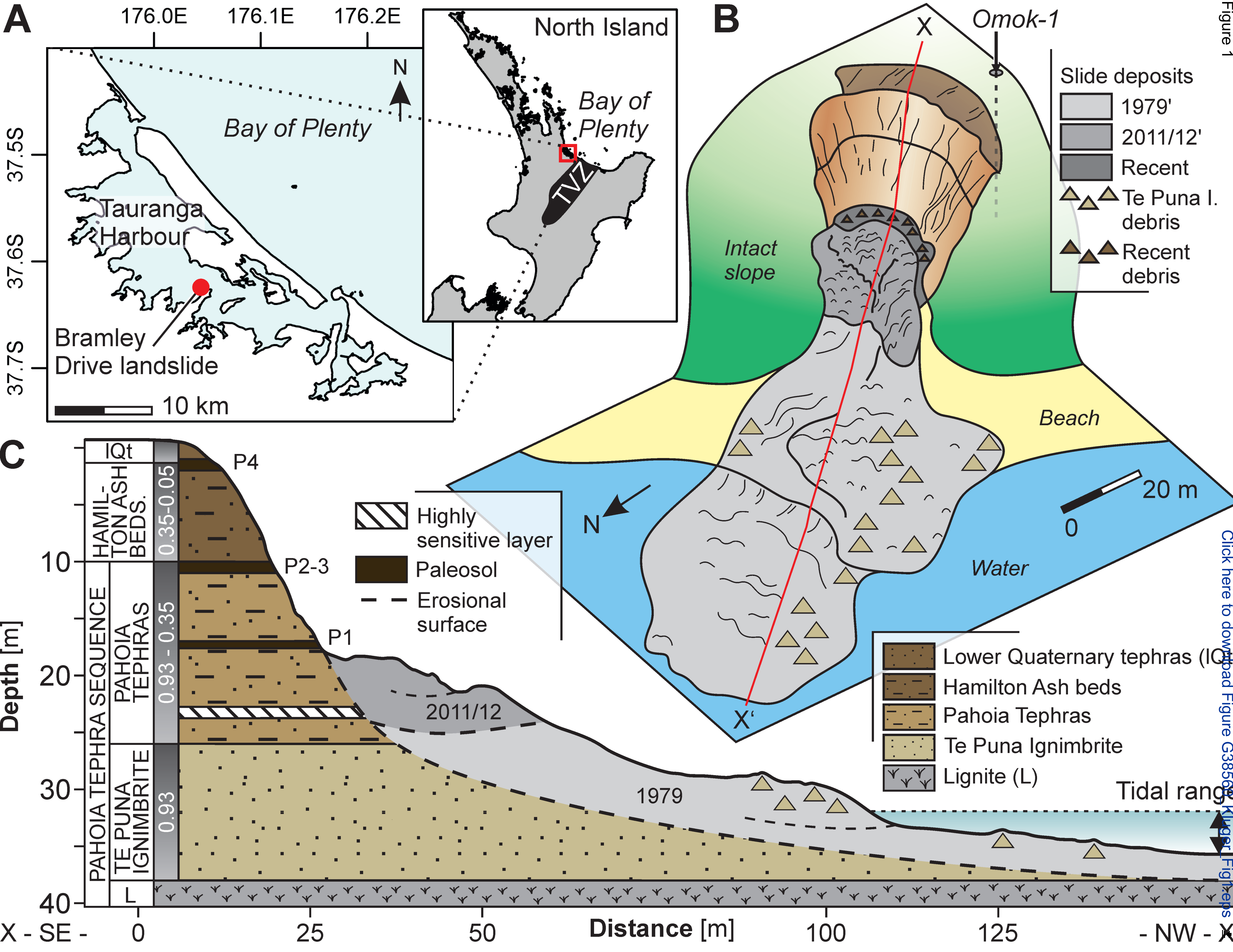

A
176.0E
176.1E
176.2E
37.5S
37.6S
37.7S
N
Bay of Plenty
Tauranga Harbour
Bramley Drive landslide
10 km
North Island
Bay of Plenty
TVZ
B
X
Omok-1
Slide deposits
1979'
2011/12'
Recent
Te Puna I. debris
Recent debris
Intact slope
Beach
Water
N
20 m
0
X'
Lower Quaternary tephras (lQt)
Hamilton Ash beds
Pahoia Tephras
Te Puna Ignimbrite
Lignite (L)
C
lQt
HAMIL-TON ASH BEDS.
0.35-0.05
PAHOIA TEPHRA SEQUENCE
PAHOIA TEPHRAS
0.93 - 0.35
TE PUNA IGNIMBRITE
0.93
L
P4
P2-3
P1
Highly sensitive layer
Paleosol
Erosional surface
2011/12
1979
Tidal range
Depth [m]
10
20
30
40
X - SE -
0
25
50
100
125
Distance [m]
- NW - X'

Figure 2

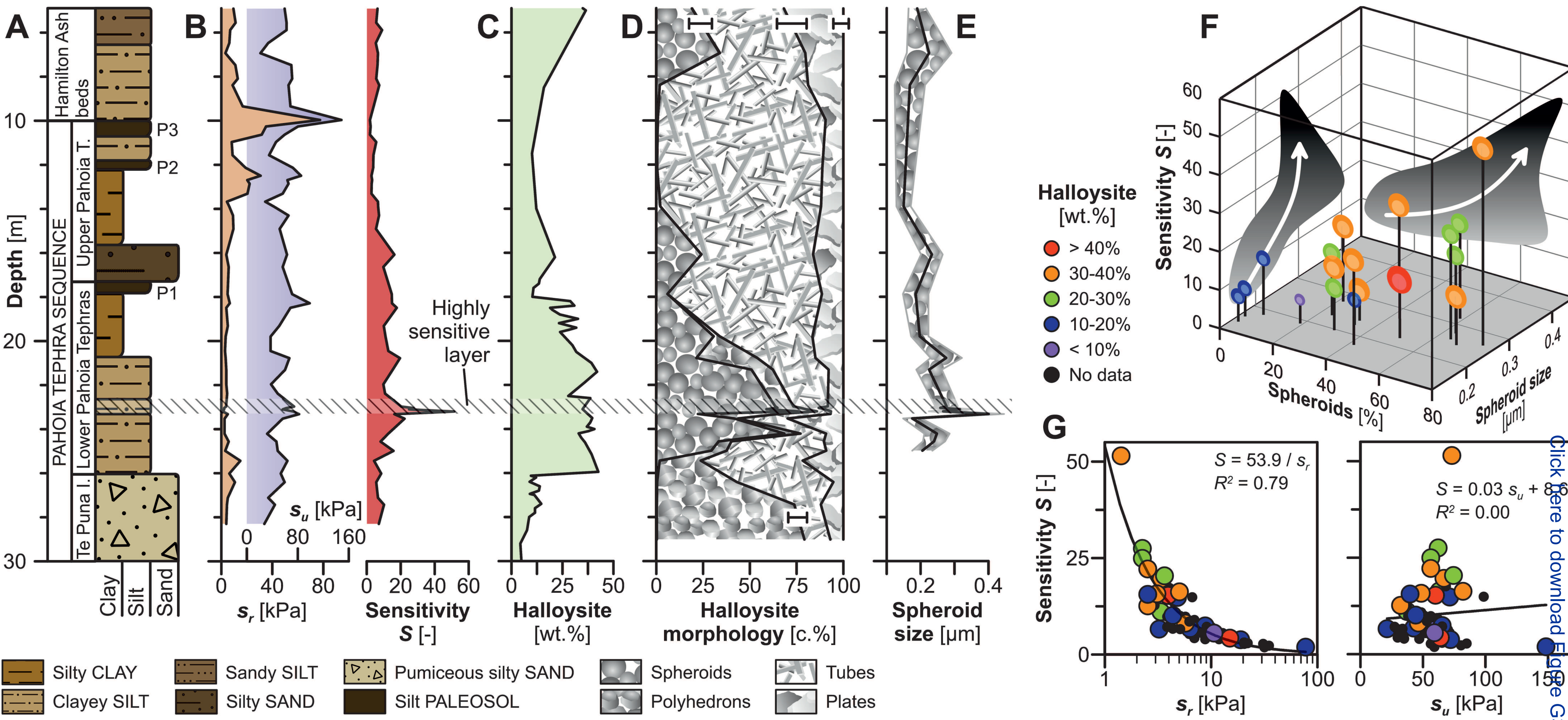
A
B
C
D
E
F
G
Depth [m]
10
20
30
Hamilton Ash beds
PAHOIA TEPHRA SEQUENCE
Upper Pahoia T.
Lower Pahoia Tephras
Te Puna I.
P3
P2
P1
Clay
Silt
Sand
s_u [kPa]
0
80
160
s_r [kPa]
0
40
80
Sensitivity
S [-]
0
20
40
60
Highly sensitive layer
Halloysite
[wt.%]
0
25
50
Halloysite morphology [c.%]
0
25
50
75
100
Spheroid size [µm]
0.2
0.4
Halloysite [wt.%]
> 40%
30-40%
20-30%
10-20%
< 10%
No data
Sensitivity S [-]
Spheroids [%]
Spheroid size [µm]
$S = 53.9 / s_r$
$R^2 = 0.79$
$S = 0.03\ s_u + 8.6$
$R^2 = 0.00$
s_r [kPa]
s_u [kPa]
Silty CLAY
Clayey SILT
Sandy SILT
Silty SAND
Pumiceous silty SAND
Silt PALEOSOL
Spheroids
Polyhedrons
Tubes
Plates

Figure 3

Click here to download Figure G38560_Kluger_Fig3.eps